Proceedings of the Jangjeon Mathematical Society
21 (2018), No. 4. pp. 745 - 758

www.jangjeon.or.kr
http://dx.doi.org/10.17777/pjms2018.21.4.745

ON THE DIFFERENT CLUSTERIZATION ALGORITHMS AND ROLE OF CROSS-SECTIONS IN FORMING COMPLEX MULTI BOUND STRUCTURES USING MONTE-CARLO SIMULATIONS

ROHIT KUMAR AND ISHITA PURI

Abstract. In the present study, we explore the role of different cluster techniques on the relative role of different cross-sections. The cluster techniques include the simple computer algorithm minimum spanning tree method based on spatial constraint and the one based on the metropolis procedure simulated annealing clusterization algorithm. We find that the relative role of different cross-sections is sensitive toward the clusterization technique used to construct complex multi-bound structures.

2010 Mathematics Subject Classification. 65Pxx, 65Zxx, 65Yxx.

Keywords and phrases. Transport model, Quantum Molecular Dynamics model, heavy-ion reactions, clusterization algorithm, Monte-Carlo Simulations, Metropolis algorithm.

1. Introduction

In last few decades, Monte-Carlo simulations are often used to solve numerically complex problems for which specific result is not known in advance. These kinds of simulations rely on repeated random sampling and statistical analysis to reproduce the results and to predict new phenomena/processes. In this direction, various complex computer programs have been developed in last couple of decades to accelerate the adoption of Monte-Carlo simulations in different fields including physics, chemistry, mathematics, engineering, finance to mention a few.

In theoretical nuclear physics, Monte-Carlo simulations are used quite often to model various phenomena occurring in heavy-ion collisions e.g., fusion, fission, multifragmentation, which are complex bound structures and need many-body correlations [1, 2, 3, 4, 5, 6, 7]. Among all these phenomena, the multifragmentation is the most crucial phenomenon that occurs over wide spectra of incident energy.

In a typical reaction, one first generates stable nuclei close to ground state using Monte-Carlo procedure and sampling [4, 7]. Care is taken so that quantum features are incorporated in a reasonable fashion and basic physics principles are not violated. Once nuclei are generated, projectile is bombarded at a given incident energy on the target. One, therefore, needs dynamical transport model which should be capable of following the reaction from the well separated target and projectile to the final state where one has multibound structures in terms of fragments of different sizes. Note that during the course of the time evolution, the size, content and number of complex bounded entities keep on changing. Such complex reaction evolution

is often divided into two steps: i) evolution of single nucleons [4, 7, 8, 9] and then ii) construction/identification of complex bound structures [7, 10, 11, 12, 13, 14, 15, 16, 17, 18, 19, 20].

It is worth mentioning that these kind of studies are not limited to physics alone, but has role in many different branches of research. In a nuclear reaction, the evolution of dynamics of individual nucleons is done by dividing reaction time into thousands of smaller steps. In between each time step, nucleons propagate using standard classical equations of motion with different kind of potentials. At the end of each time step, nucleons are screened for possible hard collisions in terms of scattering (via nucleon-nucleon cross-section). Once phase-space of nucleons is stored over entire reaction time, then using secondary clusterization algorithm, one constructs multi-particle bound structures (fragments). The problem is that several forms have been given in the literature for nucleon-nucleon cross-section [21, 22, 23] and similar is the fate of secondary algorithms [7, 10, 11, 12, 13, 14, 15, 16, 17, 18, 19, 20]. Both these are found to affect the content, size and number of complex bound fragments. We shall present here our investigation regarding the relative effect of couple of forms of cross-sections using different clusterization algorithms to ascertain whether role of different forms of cross-section is universal or is just an artifact due to choice of a particular clusterization algorithm for detecting multibound structure.

In section 2, we present the details of transport model and different clusterization algorithms. Our results are presented in section 3. Lastly, we will conclude our work in section 4.

2. Methodology

2.1. **Transport Model.** The phase space information of nucleons is generated using transport model namely, Quantum Molecular Dynamics (QMD) model [7, 24, 25]. In this model, microscopic information of nucleons is generated using interplay between potentials and binary cross-sections. The mean field comprises of three main terms namely Skyrme, Yukawa and Coulomb. During the course of the reaction, if two nucleons are close enough, they will be scattered elastically or inelastically depending on the available nucleon-nucleon cross-section [21, 22, 23]. In the present case, we will use constant cross-sections with two extreme strengths of 20 and 55 mb. As discussed in the introduction, the phase space information generated using the QMD model is stored at several time steps. The clusterization algorithms are then injected with this input to obtain fragment information. In the present study, the following clusterization algorithms are used.

2.2. **Clusterization Algorithms.** While enforcing identification of clusters, we shall compare following two algorithms:

(i) The one where clusters are formed based on the spatial proximity of the constituent nucleons. This kind of fragment or complex multibound structure algorithm is also labelled as minimum spanning tree (MST) method [7, 24, 25]. The minimum spanning tree (MST) method is the simplest and widely used algorithm. Its principle is based on checking the spatial correlations among nucleons. It is well known that after the compression phase of a reaction is over, the system proceeds towards expansion and relative difference between nucleons increases. Then

according to MST method, after certain time only those nucleons will be close to each other which are bound to each other. The nucleons i, j, k,.., are said to form a fragment C, if,

$$i \in C;\ \exists\ j \in C \mid \mathbf{r}_{ij} \leq R_{cut}, \tag{1}$$

where $\mathbf{r}_{ij} = |\mathbf{r}_i - \mathbf{r}_j|$; $\mathbf{r}_i$, $\mathbf{r}_j$ denotes the coordinates of the nucleons 'i' and 'j', respectively. R_{cut} is an arbitrary parameter whose value varies between 3-5 fm and
(ii) The second category of the method is based on the energy minimization where group of nucleons constitute fragments according to the energy (binding energy) rather than their proximity in the space. The advantage of such method is that it will not detect spurious fragments which are accidently there because of spatial proximity. Rather, it can detect fragments even if they overlap in space. Among these methods, we will use the one based on the technique of simulated annealing. This method is often labelled as Early Cluster Recognition Algorithm (ECRA) or Simulated Annealing Clusterization Algorithm (SACA) [18, 19]. The starting point of this method is any arbitrary initial configuration from which one constructs new fragment configuration by transferring (not physically) one nucleon or a set of nucleons among various fragments. If initial configuration is C_a with set of clusters:

$$C_a = \{c_1, c_2, c_3, c_4., c_n\}; \tag{2}$$

and new generated configuration is C_b with cluster set:

$$C_b = \{c'_1, c'_2, c'_3, c'_4, ., c'_n\}. \tag{3}$$

Then, the total energy of fragment configuration C_a (E_a) and C_b (E_b) is calculated. According to modelling of SACA, if

$$E_a - E_b < 0, \tag{4}$$

new cluster set C_b is accepted, otherwise accepted with finite Monte-Carlo probability to get rid of local minima. All cluster configurations C_a, C_b, C_c,. are constructed in such a way that it leads the system towards global energy minima. At the end of the simulations, we will have a cluster set C_k with maximum binding energy. This method is based on metropolis procedure; therefore, required time is much larger compared to the spatial correlation method.

It should be noted here that spatial correlation method is a local method and can be applied to a small set of entrance channels. On the other hand, SACA is a global one and can be applied to any entrance channel region. The range of applicability we mention here is decided according to the capability of secondary algorithm to reproduce experimental data [6, 18, 19, 26]. For the further discussion, we label MST and SACA methods as CA1 and CA2, respectively.

3. Results and Discussion

For the present investigations, we simulated the reactions of ^{129}Xe + ^{119}Sn at incident energies of 100 and 400 MeV/nucleon over entire colliding geometry. Here soft equation of state is employed with cross-section of 20 and 55 mb (labelled CS1 and CS2, respectively). The reactions are followed till 300 fm/c time. The MST (CA1) method sort out final fragment configuration at 300 fm/c; the time at which fragments are well separated from each other and do not change their structure. On the other hand, SACA (CA2) being based on the metropolis procedure can sort out fragments well before they are separated in coordinate space. Therefore, final fragment structure in SACA (CA2) is assumed to be at 60 fm/c.

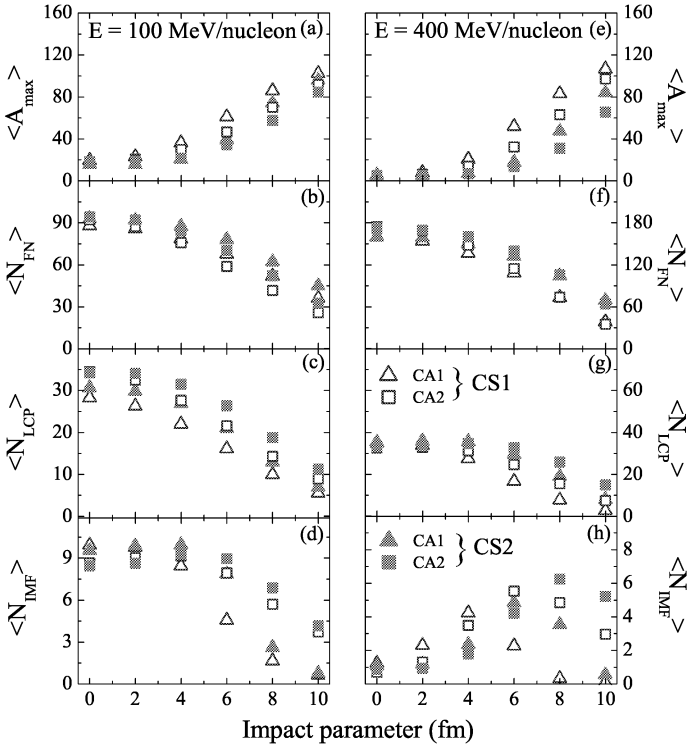

FIGURE 1. The impact parameter dependence of the size of the largest fragment $< A_{max} >$ and the multiplicities of free nucleons, LCPs and IMFs for the reaction of ^{129}Xe+^{119}Sn at 100 MeV/nucleon (left panels) and 400 MeV/nucleon (right). The open (filled) triangles and open (filled) squares represent the results of CA1 and CA2 using CS1 (CS2) cross-sections.

In Fig. 1, we display the mean size of the largest fragment ($< A_{max} >$) and multiplicities of free nucleons (<

N_{FN} >) [1≤A$_f$≤1], and multibound fragments divided into mass windows as light charged particles (< N_{LCP} >) [2≤A$_f$≤4] and intermediate mass fragments (< N_{IMF} >)) [5≤A$_f$≤30%A_{Tot}; where A_{Tot}=A_P+A_T: A_P (A_T) is the mass of projectile (target)]. The collisions are performed at incident energies of 100 (left panels) and 400 MeV/nucleon (right panels) over complete impact parameter range. Open (filled) triangles and open (filled) squares represent results obtained using CA1 and CA2 method, respectively, when CS1 (CS2) is implemented.

From the figure, we see that the size of < A_{max} > increases with impact parameter that happens due to decrease in the violence of the reaction. This increase in the value of < A_{max} > causes decrease in the multiplicity of FNs, LCPs and IMFs as a function of impact parameter (except for IMFs at 400 MeV/nucleon, where rise and fall behavior is observed). We observe that the trends are almost same for both calculations using CA1 (triangles) and CA2 (squares) methods, although, their values differ significantly. This difference between CA1 and CA2 results is already reported in literature and our results are consistent with these studies [6, 19]. Now, if we compare calculations with cross-section value of CS1 with CS2, we see that the size of < A_{max} > is large for former case compared to latter value of cross-section both for CA1 and CA2 calculations. This is well known fact that with increase in the cross-section, the size of < A_{max} > decreases and multiplicity of FNs and LCPs increases. The larger value of cross-section leads the breakage of largest fragment and thus increases the multiplicity of < N_{FN} > and < N_{LCP} >. In the case of < N_{IMF} >, the relative difference between CS1 and CS2 do not show same trends at all impact parameters using both CA1 and CA2. The value of < N_{IMF} > is larger with CS1

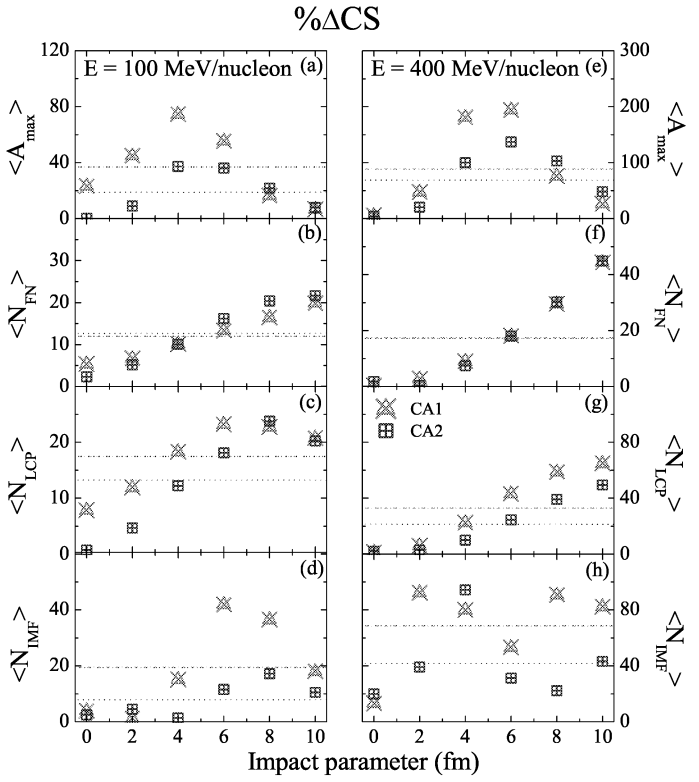

FIGURE 2. The relative % difference between the size of the largest fragment $< A_{max} >$ and the multiplicities of free nucleons, LCPs and IMFs for the reaction of ^{129}Xe+^{119}Sn at 100 MeV/nucleon (left panels) and 400 MeV/nucleon (right) at different impact parameters using CS1 and CS2, respectively. The crossed triangles (squares) represent the calculations using CA1 (CA2) method. The dash-dotted and dotted lines represent the values of relative percentage differences averaged over all impact parameters for CA1 and CA2, respectively.

compared to CS2 upto semi-peripheral geometries whereas trends get reversed at peripheral geometries. These trends are preserved with both CA1 and CA2. It is worth mentioning here that similar trends are obtained in Ref. [27], where Puri *et al* used different forms of cross-sections using CA1 as fragment identifier.

To understand the relative difference between fragment numbers using CA1 and CA2, we plot in Fig. 2, the relative percentage difference between values of $< A_{max} >$, $< N_{FN} >$, $< N_{LCP} >$ and $< N_{IMF} >$ using both CS1 and CS2 cross-sections. The relative percentage difference is calculated using following formula:

$$\%\Delta CS = \left| \frac{\sigma_{CS1} - \sigma_{CS2}}{\sigma_{CS2}} \right| \times 100. \tag{7}$$

Here crossed triangles (squares) represent relative percentage difference between fragment numbers using CA1 (CA2) method implementing CS1 and CS2 values in the QMD code. From the figure, we see that the relative percentage difference between CS1 and CS2 is less when algorithm based on metropolis procedure is used. It is important to note here that the $< A_{max} >$ and $< N_{IMF} >$ show larger difference in the calculations using CA1 and CA2. Between these, $< A_{max} >$ can shed light on the influence of cross-section to break correlations between nucleons and $< N_{IMF} >$ is termed to be crucial not only to test the predictability of model but also to understand the reason for multifragmentation. We have also plotted the relative percentage difference between CS1 and CS2 averaged over all impact parameters. Dash-dotted and dotted lines represent values obtained for CA1 and CA2, respectively. These lines clearly depict that the value of relative percentage difference averaged over impact parameters is lesser for CA2

compared to CA1, reflecting the lesser sensitivity of former compared to latter towards different forms of cross-sections.

Also, note that the relative percentage difference between calculations with CS1 and CS2 values using CA1 and CA2 pose a serious questions to all the earlier studies, where physics was conducted on cross-section based on CA1 (MST method) [21, 22, 23]. This is also supported by the recent studies done in Refs. [6, 18, 19, 26] . In these studies, we have shown that CA1 (MST method) has a very limited region of applicability, therefore, should not be used for all entrance channel parameters. On the other hand, the CA2 (SACA method) can be used for any entrance channel parameters. With these calculations in hand, we can say that systematic study is required to understand more about the cross-section values using CA2 (SACA method) as clusterization algorithm. As fragments obtained using SACA method are more close to reality, therefore, can pose better picture of cross-section in heavy-ion reaction dynamics. Studies are in progress in this direction.

4. Summary

Here we presented the calculations of nuclear reactions with different reaction cross-sections using two different clusterization algorithms. Our study shows that the effect of different extreme cross-sections is minimized with metropolis based clusterization algorithm.

References

[1] M. B. Tsang *et al., Onset of Nuclear Vaporization in* $^{197}Au+^{197}Au$ *Collision*, Phys. Rev. Lett. 71 (1993), 1502.

[2] A. Schüttauf *et al., Universaility of spectator fragmentation at relativistic bombarding energies*, Nucl. Phys. A 607 (1996), 457.

[3] W. J. Llope *et al., Auto correlations and intermediate-mass-fragment multiplicities in central heavy-ion collisions*, Phys. Rev. C 51 (1995), 1325.

[4] G. F. Peaslee *et al., Energy dependence of multifragmentation in* $^{84}Kr+^{197}Au$ *collisions*, Phys. Rev. C 49 (1994), R2271.

[5] B. Borderie *et al., Nuclear multifragmentation and phase transition for hot nuclei*, Prog. Part. and Nucl. Phys. 51 (2008), 551.

[6] Y. K. Vermani *et al., Microscopic approach to the spectator matter fragmentation from 400 to 1000 MeV/nucleon*, Euro. Phys. Lett. 85 (2009), 62001.

[7] J. Aichelin *et al., Quantum molecular dynamic: A dynamical microscopic n-body approach to investigate fragment formation and the nuclear equation of state in heavy-ion collisions*, Phys. Rep. 202 (1991), 233; R. K. Puri *et al., Temperature-dependent mean field and its effect on heavy-ion reactions*, Nucl. Phys. A 575 (1994), 733.

[8] W. Bauer *et al., Energetic photons from intermediate energy proton- and heavy-ion-induced reactions*, Phys. Rev. C 34 (1986), 2127.

[9] T. Gaitanos, H. Lenske and U. Mosel, *Fragment formation in proton induced reactions within a BUU transport model*, Phys. Lett. B 663 (2008), 197; O. Buss *et al., Transport-theoretical description of nuclear reactions*, Phys. Rep. 512 (2012), 1.

[10] S. Kumar and R. K. Puri, *Role of momentum correlations in fragment formation*, Phys. Rev. C 58 (1998), 320; J. Singh and R. K. Puri, *Study of the formation of fragments with different clusterization methods*, J. Phys. G: Nucl. Part. Phys. 27 (2001), 2091.

[11] S. Kumar and R. K. Puri, *Stability of fragments formed in the simulations of central heavy ion collisions*, Phys. Rev. C 58 (1998), 2858; S. Goyal and R. K. Puri, *Formation of fragments in heavy-ion collisions using a modified clusterization method,* Phys. Rev. C 83 (2011), 047601.

[12] S. Pratt, C. Montoya and F. Romming, *Balancing nuclear matter between liquid and gas*, Phys. Lett. B 349 (1995), 261; J. Pan and S. D. Gupta, *Unified description for the nuclear equation of state and fragmentation in heavy-ion collisions*, Phys. Rev. C 51 (1995), 1384.

[13] R. Kumar, S. Gautam and R. K. Puri,*Multifragmentation within a clusterization algorithm based on thermal binding energies*, Phys. Rev. C 89 (2014), 064608 ; ibid. *Influence of different binding energies in clusterization approach: fragmentation as an example*, J. Phys. G: Nucl. Part. Phys. 43 (2016), 025104.

[14] Y. Zhang *et al., Effect of isospin-dependent cluster recognition on the observables in heavy ion collisions*, Phys. Rev. C 85 (2000), 051602.

[15] C. Ngo *et al., Dynamical instability of hot and compressed nuclei*, Nucl. Phys. A 499 (1989), 148.

[16] R. J. Charity *et al., Systematics of complex fragment emission in niobium-induced reactions*, Nucl. Phys. A 483 (1988), 371; L .Wang *et al., Transverse momentum distributions in intermediate-energy heavy-ion collisions*, Nucl. Phys. A 920 (2013), 1.

[17] J. P. Bondorf *et al., Statistical multifragmentation of nuclei: (I). Formulation of the model*, Nucl. Phys. A 443 (1985), 321; D. H. E. Gross, *Statistical decay of very hot nuclei-the production of large clusters*, Rep. Prog. Phys. 53 (1990), 605 and references therin; H. W. Barz *et al., Charged-particle correlations in 600 AMeV gold induced disassembly reactions, a statistical multifragmentation analysis*, Nucl. Phys. A 561 (1993), 466.

[18] C. Dorso *et al., Early recognition of clusters in molecular dynamics model*, Phys. Lett. B 301 (1993), 328.

[19] R. K. Puri *et al., Simulating annealing clusterization algorithm for studying the multifragmentation*, J. Comput. Phys. 162 (2000), 245; J. Phys. G: Nucl. Part. Phys. 37 (2010), 015105; R. K. Puri *et al., Early fragment formation in heavy-ion collisions*, Phys. Rev C 54 (1996), R28.

[20] A. Le Fevre, Y. Leifels, J. Aichelin, C. Hartnack, V. Kireyev and E. Bratkovskaya, *FRIGA, a new approach to identify isotopes and hypernuclei in n-body transport models*, J. Phys. Conf. Ser. 668 (2016), 012021.

[21] H. W. Barz *et al., Cluster production and correlations in nuclear molecular dynamics*, Phys. Lett. B 382 (1996), 343; G. F. Bertch *et al., Transverse momentum distributions in intermediate-energy heavy-ion collisions*, Phys. Lett. B 189 (1987), 384.

[22] J. Cugnon *et al., Medium effects in the nuclear Landau-Vlassov transport theory*, Phys. Rev. C 35 (1987), 861; D. Klakow *et al., Nuclear flow excitation function*, Phys. Rev. C 48 (1993), 1982.

[23] G. D. Westfall *et al., Mass Dependence of the Disappearance of Flow in Nuclear Collisions* , Phys. Rev. Lett. 71 (1993), 1986; D. J. Magestro *et al., Disappearance of transverse flow in Au + Au collisions*, Phys. Rev. C 61 (2000), 021602.

[24] R. K. Puri, S. Kumar, *Binary breakup: Onset of multifragmentation and vaporization in Ca-Ca collisions*, Phys. Rev. C 57 (1998), 2744.

[25] J. Singh, S. Kumar and R. K. Puri, *Momentum dependent interactions and the asymmetry of the reaction: Multifragmentation as an example*, Phys. Rev. C 63 (2001), 054603; S. Kumar and R. K. Puri, *Importance of momentum dependent interactions in multifragmentation*, Phys. Rev. C 60 (1999), 054607.

[26] R. Kumar, Ph. D. thesis, Panjab University, Chandiagrh, 2016 (unpublished).

[27] S. Kumar *et al., Different nucleon-nucleon cross sections and multifragmentation*, Phys. Rev. C 58 (1998), 1618; J. Singh, S. Kumar and R. K. Puri, *Model ingredients and multifragmentation in symmetric and asymmetric heavy ion collisions*, Phys. Rev. C 62 (2000), 044617.

Department of Physics, Panjab University, Chandigarh - 160014, India

E-mail address: rohitksharma.pu@gmail.com

Department of Information Technology, UIET, Panjab University,, Chandigarh-160014, India

E-mail address: ishitapuri.work@gmail.com